JOURNAL OF PROTEOMICS 94 (2013) 311–326

Available online at www.sciencedirect.com

ScienceDirect

www.elsevier.com/locate/jprot

Conserved Asf1–importin β physical interaction in growth and sexual development in the ciliate *Tetrahymena thermophila*☆

Jyoti Garg[a], *Jean-Philippe Lambert*[b,1], *Abdel Karsou*[c,1], *Susanna Marquez*[a], *Syed Nabeel-Shah*[c], *Virginia Bertucci*[a], *Dashaini V. Retnasothie*[a], *Ernest Radovani*[c], *Tony Pawson*[b,d], *Anne-Claude Gingras*[b,d], *Ronald E. Pearlman*[a], *Jeffrey S. Fillingham*[c,*]

[a]*Department of Biology, York University, 4700 Keele St., Toronto M3J 1P3, Canada*
[b]*Lunenfeld-Tanenbaum Research Institute, Mount Sinai Hospital, 600 University Avenue, Toronto M5G 1X5, Canada*
[c]*Department of Chemistry and Biology, Ryerson University, 350 Victoria St., Toronto M5B 2K3, Canada*
[d]*Department of Molecular Genetics, University of Toronto, Toronto M5S 1A8, Canada*

ARTICLE INFO

Article history:
Received 30 May 2013
Accepted 23 September 2013
Available online 11 October 2013

Keywords:
Tetrahymena
Asf1
Proteomics
Chromatin

ABSTRACT

How the eukaryotic cell specifies distinct chromatin domains is a central problem in molecular biology. The ciliate protozoan *Tetrahymena thermophila* features a separation of structurally and functionally distinct germ-line and somatic chromatin into two distinct nuclei, the micronucleus (MIC) and macronucleus (MAC) respectively. To address questions about how distinct chromatin states are assembled in the MAC and MIC, we have initiated studies to define protein–protein interactions for *T. thermophila* chromatin-related proteins. Affinity purification followed by mass spectrometry analysis of the conserved Asf1 histone chaperone in *T. thermophila* revealed that it forms a complex with an importin β, ImpB6. Furthermore, these proteins co-localized to both the MAC and MIC in growth and development. We suggest that newly synthesized histones H3 and H4 in *T. thermophila* are transported via Asf1–ImpB6 in an evolutionarily conserved pathway to both nuclei where they then enter nucleus-specific chromatin assembly pathways. These studies set the stage for further use of functional proteomics to elucidate details of the characterization and functional analysis of the unique chromatin domains in *T. thermophila*.

Biological significance
Asf1 is an evolutionarily conserved chaperone of H3 and H4 histones that functions in replication dependent and independent chromatin assembly. Although Asf1 has been well studied in humans and yeast (members of the Opisthokonta lineage of eukaryotes), questions remain concerning its mechanism of function. To obtain additional insight into the Asf1 function we have initiated a proteomic analysis in the ciliate protozoan *T. thermophila*, a member of the Alveolata lineage of eukaryotes. Our results suggest that an evolutionarily conserved function of Asf1 is mediating the nuclear transport of newly synthesized histones H3 and H4.

☆ This paper is dedicated to the memory of Dr. Tony Pawson who recently passed away unexpectedly.

* *Corresponding author at:* Department of Chemistry and Biology, Ryerson University, Toronto M5B 2K3, ON, Canada. Tel.: +1 416 979 5000x2123.
E-mail address: jeffrey.fillingham@ryerson.ca (J.S. Fillingham).

[1] Equal contribution.

1874-3919/$ – see front matter
http://dx.doi.org/10.1016/j.jprot.2013.09.018

1. Introduction

Chromatin assembly is the process by which the nucleosome is formed. Replication-dependent (RD) chromatin assembly is co-ordinated with chromosomal replication and is an important mechanism underlying epigenetic regulation. This includes maintenance of patterns of gene expression via faithfully replicating parental patterns of histone post-translational modifications (PTMs) onto the daughter strand [1]. Replication Independent (RI) chromatin assembly pathways occur independent of chromosomal replication at any time within the cell cycle and contribute to chromatin remodeling by a selective insertion of histone variants such as histone H3.3 in human cells [2]. Increasingly, connections are being found between mutations in genes encoding RD or RI chromatin assembly proteins, histones themselves, and a variety of human diseases [3–9]. However a complete understanding of how chromatin assembly proteins contribute to the establishment, remodeling, and epigenetic maintenance of chromatin structure is lacking.

Histone chaperones are proteins that bind histones, are involved in their assembly onto chromatin, but are not themselves part of chromatin [2]. The conserved histone H3–H4 chaperone Asf1 has a central role in eukaryotic chromatin assembly. ASF1 was first isolated as a gene that when over-expressed, de-repressed the yeast silent mating type locus [10]. Asf1 was mechanistically connected to the chromatin assembly when the in vitro replication-coupling assembly factor activity (RCAF) was identified as Asf1 bound to histones H3 and H4 (Asf1–H3–H4) [11]. ASF1 has been implicated in a wide variety of functions that range from transcription activation [12] and repression [13] to maintenance of genome stability [14], DNA replication [15], DNA repair [16], and cellular aging [17]. The mechanism by which Asf1 functions in *Saccharomyces cerevisiae* is explainable in part by its role in the promotion of acetylation of histone H3 at lysine 56 (H3-K56ac), which is catalyzed by the fungal-specific histone acetyltransferase (HAT) Rtt109 [18–20] in conjunction with Asf1^{Sc} [21]. The enzymology behind H3K56ac in human cells is more complex with several HATs implicated including CBP/p300 [4,22] and Gcn5^{Hs} [23]. The knock-down of Asf1A but not Asf1B in human cells decreases levels of H3K56ac [4].

The Asf1 function has also been revealed by the identification and characterization of Asf1 protein–protein interaction partners. In *S. cerevisiae*, Asf1 (Asf1^{Sc}) co-purifies with a number of proteins including the Rad53 checkpoint kinase [24], the HIR histone H3–H4 RI chaperone complex [25,26], the nuclear Hat1 complex [27] as well as histones H3 and H4. In human cells, epitope tagged Asf1a^{Hs} co-purifies with several proteins including the disease-related Codanin protein, Importin-4, sNASP, RbAp46/48, MCM 2–7 replicative helicase [5,28], histone H4 and the RD H3.1 and RI H3.3 [29]. Codanin was recently demonstrated to directly bind Asf1 and negatively regulate importin-4 mediated transport of Asf1–H3–H4 into the nucleus [5]. These human protein–protein interactions have led to a model where Asf1 binds newly synthesized H3–H4 in the cytoplasm, and transports them into the nucleus in complex with importin-4 regulated by codanin [5,30]. The Hat1 complex, consisting of Hat1, Hat2 (human RbAp46/48) and Hif1 (human NASP) [27,30], has been proposed to act upstream of the H3–H4 binding by Asf1 in the cytoplasm, possibly influencing the interaction of importin-4 with Asf1–H3–H4 [31,32].

Once in the nucleus, Asf1 transfers the H3–H4 dimer to downstream RI and RD H3–H4 chaperones HIRA, and CAF-1. The yeast version of HIRA is a protein complex of Hir1, Hir2, Hir3 and Hpc2 [26]. Human HIRA has high similarity in sequence and function to both Hir1p and Hir2p [33]. Human orthologs of Hir3 (CABIN1) and Hpc2 (Ubinuclein) have been identified to also bind H3.3 with HIRA [34]. HIRA is hypothesized to assemble H3.3–H4 into chromatin in a poorly understood replication independent manner. CAF-1 is composed of Cac1, Cac2, and Cac3 subunits [35]. CAF-1 is thought to function in chromatin assembly by sequentially accepting two H3–H4 dimers, one parental and one newly synthesized, which it then assembles as a tetramer behind the replication fork [36]. CAF-1 assembles H3–H4 into chromatin at the replication fork in a manner coordinated by a physical interaction with the PCNA loading clamp [37]. Asf1 physical interaction with CAF-1 and HIRA is well characterized in vitro. Both CAF-1 p60 and HIRA physically interact in a mutually exclusive manner with the same region in human and yeast Asf1, separate from its H3–H4-binding region. Despite this model, questions remain concerning the mechanism of action of Asf1. The importin-4 mediated Asf1a–H3–H4 nuclear import is highly regulated in human cells. An analogous pathway in yeast likely exists with Kap123 mediating import of Asf1–H3–H4. However the physical interaction appears transient in that it is not easily detected, and the absence of a Codanin related protein suggests that the importance of this pathway may be different.

The single-cell ciliate protozoan *Tetrahymena thermophila* offers an experimental system well-suited to unravel some of the questions concerning Asf1 mechanism and function. The *T. thermophila* model features a separation of structurally distinct germ-line and somatic chromatin into two distinct nuclei, the micronucleus (MIC) and macronucleus (MAC) that are both present in a single cell (reviewed in [38]). Functionally, the somatic polyploid MAC controls gene expression, and the germinal diploid MIC controls stable genetic inheritance. These two functionally and spatially distinct nuclei originate during sexual development from the same zygotic nucleus, but then follow distinct developmental pathways whose chromatin organization share important similarities with the epigenetic changes that occur to mammalian chromatin during development. Although *T. thermophila* is rich in the H3K56ac PTM [39], it does not encode recognizable homologs of *RTT109* or human CBP begging the question — what is the identity of its H3K56ac HAT? Starting with a proteomics work-flow, we present the affinity purification, subsequent characterization, and functional analysis of chromatin-related protein complexes containing the histone H3–H4 chaperone Asf1 in *T. thermophila*. Asf1 is conserved in eukaryotes and has a canonical function upstream of both RD and RI chromatin assembly. Affinity purification of *T. thermophila* Asf1 followed by mass spectrometry analysis reveals that it forms a protein complex with an importin β, ImpB6. Our analysis indicates that Asf1 and ImpB6 co-localize to both the MAC and MIC in growing cells. We suggest that newly synthesized H3 and H4 in *T. thermophila* in growth and development are funneled through Asf1–ImpB6 to both the MAC and MIC. Histones H3 and H4 then enter nucleus-specific chromatin assembly pathways.

2. Results

2.1. ASF1 is conserved in T. thermophila

We initiated our analysis of Asf1^{Tt} by using BLASTX to search the sequenced macronuclear genome [40] using the Asf1^{Sc} amino acid sequence (GenBank AAC37512). We found one high-confidence match, TTHERM_00442300, hereafter called ASF1^{Tt}, indicating that ASF1^{Tt} is a single-copy gene. Gene prediction model of the *Tetrahymena* Genome Database (TGD, www.ciliate.org) indicates no introns and a predicted coding region of 756 bp encoding a protein of 251 amino acids. We used multiple sequence alignment to compare Asf1^{Tt} with Asf1 from several well-characterized models. In this alignment we used only the first 156 of the 251 amino acids of Asf1^{Tt} which corresponds to amino acids 1–155 of Asf1^{Sc}, also referred to as Asf1N [41]. As with other organisms, the C-terminal sequence of Asf1^{Tt} is not well conserved. The best match to Asf1^{Tt} (Fig. 1A) was that of the closely related ciliate and freshwater fish ectoparasite *Ichthyophthirius multifiliis* at 83% identity. The related ciliate *Paramecium tetraurelia* (data not shown) encodes 10 Asf1 proteins, a consequence of multiple whole genome duplications [42]. The Asf1N region of Asf1^{Tt} is 41%/43% identical to Asf1 of budding/fission yeast, and 44%/42% identical to Asf1a^{Hs} and Asf1b^{Hs} respectively, the two Asf1 proteins in human cells [43]. Overlying the multiple sequence alignment (Fig. 1B) are secondary structure predictions, as well as histone

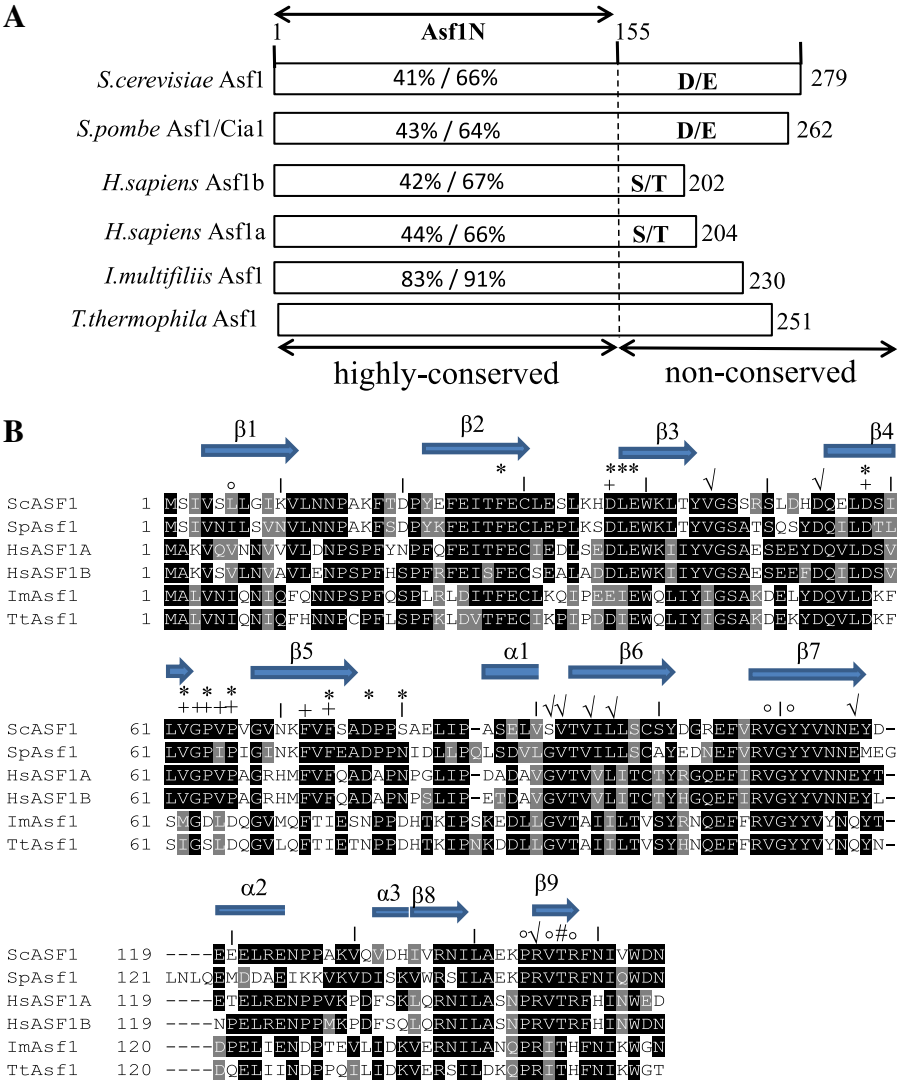

Fig. 1 – Comparative sequence analysis of Asf1^{Tt}. A: Identity/similarity of the highly conserved Asf1N region (corresponds to amino acids 1–155 of Asf1 of *S. cerevisiae*) between several model Asf1 proteins. D/E indicates that the region is rich in aspartic and glutamic acid amino acids. S/T indicates that the region is rich in serines and threonines. B: Comparative sequence analysis of the highly conserved Asf1 N terminal region as described in the text. Accession numbers: *T. thermophila*, XP_001033143.3; *S. cerevisiae*, AAC37512.1; *S. pombe*, NP_588267.1; *H. sapiens*, EAW48193.1 (Asf1A) and AAH36521.1 (Asf1B); *I. multifiliis*, EGR28891. "∘" and "√" represent points of contact between Asf1^{Sc} and histones H4 and H3 respectively (from English et al. [44]), "+" between Asf1a^{Hs} and HIRA (Tang et al. [47]), "*" between Asf1^{Sp} and Hip1 (Malay et al. [46]). "!" indicates V94R of Asf1^{Sc} and "#" represents T148 of Asf1^{Sc} that contacts both H3 and H4 [44].

H3–H4 and CAF-1/HIR-contacting residues, as determined for Asf1^{Sc} and Asf1^{Hs} [44–47]. Asf1^{Sc} has been demonstrated to bind histone H3 through a region comprised of β-strands (β3, β4, and β6–9), and H4 primarily via the β9 strand ([44], Fig. 1B). Consistent with histone-binding function, the sequence conservation of the N-terminal region of Asf1^{Tt} with the same region in Asf1 from other eukaryotes is extensive (Fig. 1B, Supplemental Fig. 1A + B), although some deviations exist. For example, *ASF1*^{Tt} encodes histidine instead of arginine at amino acid position 149 (corresponds to 148 in Asf1^{Sc}). This amino acid contacts H4R95 [44], which is conserved in the major and minor H4 in *T. thermophila* (Supplemental Fig. 2A). Additionally, Asf1^{Sc} E116 that contacts H3K115 corresponds to Asf1^{Tt} Q117 (Fig. 1A) which is predicted to contact *T. thermophila* H3R115 (Supplemental Fig. 2B). Thus most sequence deviations within this region in Asf1^{Tt} is compensatory reflecting sequence differences in evolutionarily divergent eukaryotes.

A region within Asf1^{Tt} that is not well conserved includes β4 and β5 (Fig. 1B) implicated in Asf1 direct non-histone protein–protein interactions (PPIs). This region in Asf1^{Sc} and Asf1^{Hs} recognizes and binds a sequence called the B-domain in proteins such as CAF-1 and HIRA in a manner that does not preclude binding to H3–H4 [41,47]. Within this region, several amino acids are conserved including D37 (Fig. 1B), but there is clear divergence in the region spanning amino acids 59–66 that in humans and yeast Asf1 includes two prolines, P64 and P66 that create a hydrophobic binding pocket. In Asf1^{Tt}, these prolines are replaced by hydrophilic aspartic acid residues (Fig. 1B). We predict Asf1^{Tt} to function as a histone H3–H4 binding protein, but there may be differences in its interactions with non-histone proteins compared with yeast/metazoans.

2.2. *Proteomic analysis of Asf1^{Tt} in vegetatively growing T. thermophila*

We generated a stable line expressing Asf1^{Tt} with a C-terminal FZZ epitope tag from the MAC. The FZZ epitope tag contains 2 protein A moieties and one 3xFLAG separated by a TEV cleavage site (Fig. 2A, [48]), permitting a tandem affinity purification of the fusion protein which allows analysis of co-purifying proteins by Western blotting and/or mass spectrometry. The FZZ construct (Supplemental Fig. 3A) was used to transform growing *T. thermophila* strains using biolistic transformation. Gene replacement of the WT *ASF1*^{Tt} locus by *ASF1*^{Tt}-FZZ occurs by homologous recombination [49]. The polyploid MAC divides amitotically without equal segregation of alleles. 'Phenotypic assortment' (reviewed in [50]) of the transformed cells generates homozygocity in the polyploid MAC for the chromosome containing *ASF1*^{Tt}-*FZZ*. Southern blotting demonstrates a complete replacement of all wild type MAC copies (Supplemental Fig. 3B). Western blotting demonstrates expression of the epitope-tagged Asf1^{Tt} from whole cell extracts from both wild type and Asf1-FZZ-expressing strains subjected to tandem affinity purification (Fig. 2B, C). Tandem affinity purified Asf1^{Tt}-FZZ was first analyzed by electrophoresis through 10% SDS-PAGE, followed by silver staining. We observed two major stained protein bands not present in the mock purification from untagged cells (Fig. 2D). MALDI-TOF analysis of gel slices identified the bait protein Asf1^{Tt}, and an additional co-purifying protein TTHERM_00962200, which encodes an importin β (Fig. 2D). Because staining was faint, we performed a more sensitive gel-free LC–MS/MS based analysis on tandem affinity purified proteins in order to identify additional proteins that co-purify with Asf1^{Tt}-FZZ.

To provide statistical rigor to our AP–MS analysis, interaction data were filtered using SAINT (Significance Analysis of INTeractome) which uses quantitative spectral counts to assign a confidence value to individual protein–protein interactions [51,52]. The SAINT method assigns a probability value to an interaction based on data from both control and experimental AP–MS, taking into consideration data from biological replicates, permitting rigorous discrimination between true and false interactions. The application of SAINT to AP–MS data for Asf1^{Tt}-FZZ from vegetatively growing *T. thermophila* revealed numerous interaction partners with AvgP > 0.8 (Table 1). SAINT analysis also verified the presence of the importin β TTHERM_00962200 in the Asf1^{Tt} purification (AvgP = 1.0, Table 1) consistent with what we observed in the MALDI experiment. We also identified TTHERM_01014770 (Nrp1; NASP-related protein) with an AvgP = 1.0 (Table 1). Nrp1 is a predicted 510 amino acid protein that is similar to the *Xenopus* N1/N2 protein, the founding member of a histone chaperone family that also includes NASP^{Hs}, and Hif1^{Sc} [2]. Consistent with this observation, we have previously demonstrated that Asf1 and Hif1 co-purify in yeast [27]. In addition, Asf1 co-purifies with NASP in human cells [30,53]. The finding that Asf1 and Nrp1 physically interact in *T. thermophila* suggests an ancient origin and a fundamental function for this physical interaction in eukaryotes. SAINT analysis also revealed two additional similar Asf1^{Tt}-FZZ co-purifying proteins, THERM_00530680 (AvgP = 1.0, Table 1), and TTHERM_00565630 (AvgP = 1.0, Table 1). Both are large proteins (2226 and 2220 amino acids, respectively) that we have named Aip1 and Aip2 (Asf1-interacting proteins 1 and 2). Both Aip1 and Aip2 are similar to each other at the amino acid level and are two members of a four protein ortholog group (OG5_181825) in the orthology database OrthoMCL [54], along with the *T. thermophila* protein TTHERM_00444610 that we did not find to co-purify with Asf1^{Tt} and one *Dictyostelium discoideum* protein, abpF (Actin-binding protein F). Both Aip1 and Aip2 do not contain recognizable domains other than a single coiled coil. SAINT analysis also revealed co-purification of both TTHERM_00307700 (AvgP = 1.0, Table 1) that we have named Aip3, a protein of 40 kDa predicted molecular mass that contains an N-terminal RING domain, followed by a C-terminal tandem BRCT domain, and TTHERM_00105110 (AvgP = 1.0, Table 1), a dnak HSP70 related protein.

2.3. *Asf1 and ImpB6 are functionally linked*

The protein encoded by TTHERM_00962200 which co-purified with Asf1^{Tt}-FZZ (Fig. 2G; Table 1) is one of 11 previously identified *T. thermophila* importin β's, ImpB6 [55]. Importin β's are large (95–145 kDa) proteins composed of multiple HEAT repeats that function in the nuclear import of proteins. When bound to their cargo, importins translocate through the nuclear pore complex via transient interactions with nucleoporins. Once inside the nucleus, interaction with RanGTP causes

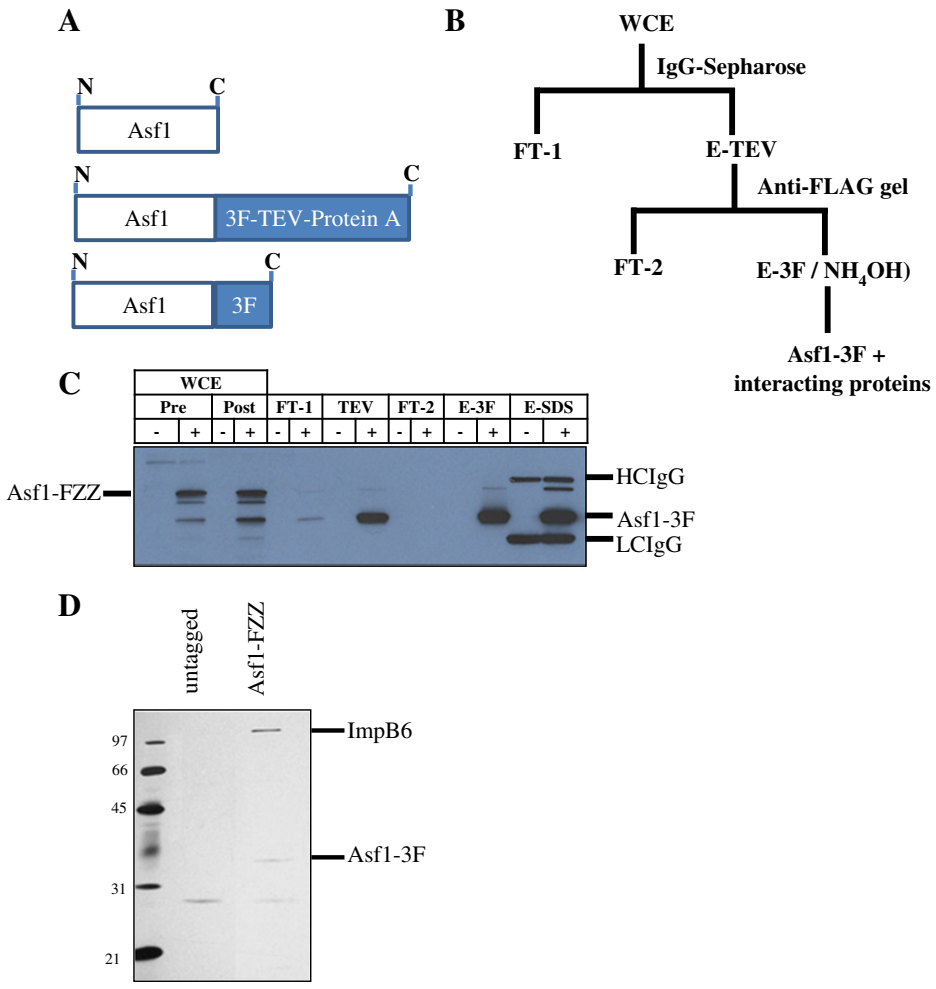

Fig. 2 – Affinity purification in *T. thermophila*. A: Comparison of WT Asf1 protein, Asf1-FZZ and Asf1-3F protein. 3F = 3xFLAG epitope tag. B: Schematic of affinity purification method. Briefly, whole cell extracts were made from ~500 ml of growing *T. thermophila* and incubated for several hours on IgG-Sepharose, cleaved overnight by TEV protease, then incubated for 2 h on M2-agarose. Elution was initially using 3xFLAG peptide and subsequently using NH_4OH. WCE = whole cell extract, FT = flow through, E = elution, 3 F = 3xFLAG peptide. C: Western blot analysis of a sample Asf1-FZZ affinity purification. Proteins separated by electrophoresis through 12% SDS-PAGE were probed using an antibody against the FLAG epitope tag (M2). D: Silver stained 10% SDS-PAGE of $Asf1^{Tt}$-FZZ eluted with 3xFLAG peptide.

dissociation of the import complex. A previous study using ectopically expressed ImpB6-GFP showed localization to both MIC and MAC, but with more intense signal observed in the MIC [55]. To further investigate ImpB6–$Asf1^{Tt}$ physical interactions, we generated a strain of *T. thermophila* carrying ImpB6-FZZ at its wild type locus. An indirect immunofluorescence of ImpB6-FZZ showed that in growing cells, ImpB6-FZZ localized to MAC and MIC (Fig. 3A), but with more intense signal observed in the MIC, consistent with previous results obtained with ectopic expression of ImpB6 [55]. Affinity purification of ImpB6-FZZ from growing cells (Fig. 3B) followed by LC–MS/MS identified a set of co-purifying proteins that was analyzed using SAINT (Table 1). The application of SAINT to AP–MS data from four ImpB6-FZZ AP–MS experiments performed on WCE made from vegetatively growing cells revealed two interaction partners with AvgP > 0.8, Aip1 (AvgP = 1.0, Table 1), and the gene product of TTHERM_00661690, a different BRCT-domain containing protein than Aip3 which only co-purifies with $Asf1^{Tt}$-FZZ. Spectral counts from Aip2 and $Asf1^{Tt}$ were identified in one of the four ImpB6-FZZ AP–MS leading to AvgP ~0.5 and MaxP (which is the highest SAINT score obtained in any given individual samples) >0.99 (Table 1). We did not observe Nrp1 or Aip3 to co-purify with ImpB6-FZZ. Two additional hypothetical proteins also co-purified with ImpB6-FZZ with MaxP > 0.8 (Table 1). In order to determine if $Asf1^{Tt}$, like ImpB6, localizes to both the MAC and MIC, we performed indirect immunofluorescence on $Asf1^{Tt}$ C-terminally tagged with GFP in growing cells. We observed localization of $Asf1^{Tt}$-GFP to both the MAC and MIC, but with more intense signal observed in the MIC similar to ImpB6-FZZ (Fig. 3A). We postulate that in growing cells, $Asf1^{Tt}$ and ImpB6 function together, along with Aip1 and Aip2. The function of these interacting proteins is likely to

Table 1 – AP-MS Data.

Bait	Prey	Gene ID	Spectral count		AvgP	MaxP
			Sample	Control		
Asf1_veg	Asf1	TTHERM_00442300	232|135|120	0|0|0|0|0|0|0|0|0|0|0	–	–
Asf1_veg	Aip1	TTHERM_00530680	208|305|119	0|0|0|0|0|0|0|0|0|0|4|0	1	1
Asf1_veg	Aip2	TTHERM_00565630	96|28|48	0|0|0|0|0|0|0|0|0|0|0|0	1	1
Asf1_veg	Aip3	TTHERM_00307700	30|4|19	0|0|0|0|0|0|0|0|0|0|0|0	1	1
Asf1_veg	DnaK	TTHERM_00105110	107|37|21	0|4|0|0|3|0|7|3|0|0|0|5|3	1	1
Asf1_veg	ImpB6	TTHERM_00962200	170|129|27	0|0|0|0|0|0|0|0|0|0|0|0	1	1
Asf1_veg	Nrp1	TTHERM_01014770	232|44|3	1|0|0|0|0|0|0|0|0|0|0|0	1	1
Asf1_6hour_conj	Asf1	TTHERM_00442300	11|10|46	0|0|0	–	–
Asf1_6hour_conj	Aip1	TTHERM_00530680	41|168|36	0|0|0	1	1
Asf1_6hour_conj	Aip2	TTHERM_00565630	15|91|7	0|0|0	1	1
Asf1_6hour_conj	Aip3	TTHERM_00307700	25|34|0	0|0|0	1	1
Asf1_6hour_conj	DnaK	TTHERM_00105110	8|12|9	6|0|0	0.51	0.59
Asf1_6hour_conj	ImpB6	TTHERM_00962200	20|25|22	0|0|0	1	1
Asf1_6hour_conj	Nrp1	TTHERM_01014770	5|0|4	0|0|0	1	1
ImportinB6_veg	ImpB6	TTHERM_00962200	27|74|80|41	0|0|0|0|0|0|0|0|0|0|0|0	–	–
ImportinB6_veg	Aip1	TTHERM_00530680	22|13|47|245	0|0|0|0|0|0|0|0|0|0|0|0	1	1
ImportinB6_veg	Aip2	TTHERM_00565630	0|0|0|87	0|0|0|0|0|0|0|0|0|0|0|0	0.5	1
ImportinB6_veg	Asf1	TTHERM_00442300	0|0|0|4	0|0|0|0|0|0|0|0|0|0|0|0	0.49	0.99
ImportinB6_veg	Brct1	TTHERM_00661690	4|2|11|0	0|0|0|0|0|0|0|0|0|0|0|0	0.99	1
ImportinB6_veg	Hypothetical 1	TTHERM_00497970	12|0|0|0	0|0|0|0|0|0|0|0|0|0|0|0	0.5	1
ImportinB6_veg	Hypothetical 2	TTHERM_00148850	0|0|0|3	0|0|0|0|0|0|0|0|0|0|0|0	0.46	0.92

AvgP calculated independently for ASF1 and ImpB6 due to larger variability prey spectral counts.

regulate the import of newly synthesized histones H3 and H4 into both the MIC and MAC where they subsequently enter replication dependent and independent pathways. In order to determine if another Asf1^{Tt}-FZZ co-purifying protein also localizes to both the MAC and MIC, we analyzed a cell line expressing Aip3-GFP (Fig. 3C) that co-purifies with Asf1^{Tt}-FZZ but not ImpB6-FZZ (Table 1). Our immunofluorescence analysis of this cell line indicates that AIP3-FZZ localizes primarily to the MIC (Fig. 3D). Thus at least one interaction partner of Asf1^{Tt} is nucleus-specific.

2.4. *Role of ASF1^{Tt} in development*

To investigate whether Asf1^{Tt} functions in *T. thermophila* development, we examined Asf1^{Tt}-FZZ expression by Western blotting of whole cell extracts made from growing, or conjugating cells. We observed expression of Asf1^{Tt}-FZZ throughout conjugation (Fig. 4A), consistent with its role during nuclear development. Note the expression pattern of the conjugation-specific Pdd1 protein (TTHERM_00125280) shown as a control, which dramatically increases during conjugation [56] (Fig. 4A). *T. thermophila* conjugation includes several nuclear developmental stages that can be monitored by indirect immunofluorescence [57]. Meiosis occurs between 2 and 4 h after mixing cells of different mating types. Meiotic prophase is characterized by the micronucleus forming an elongated crescent shape, almost twice the length of the cell. Ultimately, meiosis of the diploid MIC produces four haploid products, only one of which is retained, which then divides once mitotically and reciprocally exchanges with that of the attached conjugation partner (pronuclear exchange). These two haploid gametic nuclei in each cell fuse to produce an identical diploid zygotic nucleus in each of the conjugating cells. Between 4 and 6 h post-mixing, these zygotic nuclei divide mitotically twice, producing four genetically identical nuclei per cell. At this point separate developmental programs commence that ultimately result in two mature MIC and MAC per cell by 18 h post-mixing [57]. We conjugated two strains of different mating types both expressing Asf1^{Tt}-GFP in order to determine its localization during conjugation. Consistent with the observation in growing cells (Fig. 4B), we observed both MIC and MAC staining in samples harvested from starved cells, and during the beginning and crescent stage of meiosis (Fig. 4B–D). At both stages, Asf1-GFP staining appears more intense in the MIC than MAC. Post-meiosis, Asf1-GFP staining is observed at roughly the same levels in all four pre-zygotic nuclei around the time of pronuclear exchange (Fig. 4E). When MAC and MIC begin to look different from each other due to separate developmental programs, we again observed a stronger presence of Asf1-GFP in the MIC than in the MAC (Fig. 4F). In order to determine if Asf1 has novel functions in nuclear development, we affinity purified Asf1-FZZ from whole cell extracts made from 6 h post-mixing cells (Fig. 4G), a time period where most mating cells should have finished nuclear post-zygotic divisions. SAINT analysis of the interacting protein data set indicated no obvious quantitative difference in these post-zygotic samples, despite reduced spectral counts for Asf1^{Tt} interaction partners as compared to the growing cells, suggesting that Asf1^{Tt} interactions may be stable through nuclear division (Table 1) and Asf1^{Tt} probably functions throughout development as well as growth.

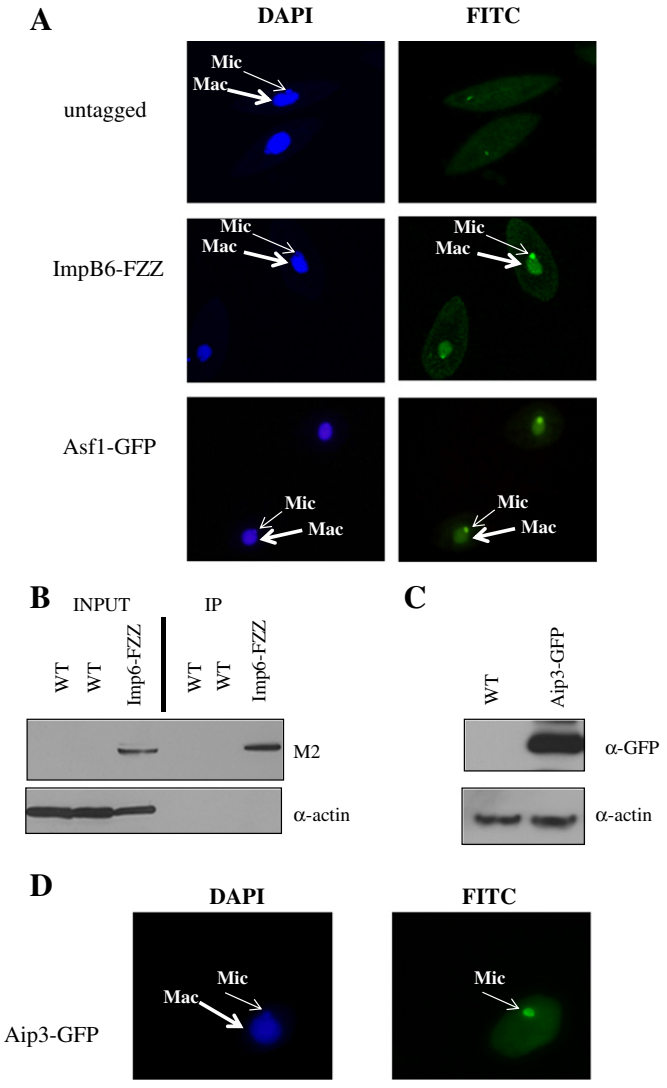

Fig. 3 – Analysis of ImpB6-FZZ. A: Indirect immunofluorescence of untagged cells and ImpB6-FZZ using M2 antibody, and Asf1-GFP using anti-GFP antibody. B: Western blotting of affinity purified ImpB6-FZZ using M2 antibody. C: Western blotting analysis of whole cell extracts made from WT and Aip3-FZZ cells using anti-FLAG antibody. α-Actin is a loading control on Western blot analysis. D: Indirect immunofluorescence of Aip3-FZZ cells using anti-GFP antibody.

2.5. *Asf1^{Tt} binds H3 and H4 in vitro*

In order to test our prediction that Asf1^{Tt} binds H3–H4 in vitro we expressed and purified recombinant full-length 6xHIS-Asf1^{Tt}. Our results using pull down experiments demonstrate that 6xHIS-Asf1^{Tt} can selectively bind histones H3 and H4 from mixtures containing histones H1, H2A, H2B, H3, and H4 purified from either chicken erythrocytes (Fig. 5A) or the *T. thermophila* macronucleus (Fig. 5B). 6xHIS-Asf1N^{Tt} (amino acids 1–156 of Asf1^{Tt}) displayed a similar ability to selectively bind histones H3 and H4 from these mixtures (Supplemental Fig. 4) suggesting that, consistent with our comparative sequence analysis (Fig. 1B), the major histone-binding region of Asf1^{Tt} resides within the evolutionarily conserved region. Thus Asf1^{Tt} binds histones H3 and H4, in agreement with its canonical function as a histone chaperone.

2.6. *ASF1^{Tt} does not compensate for the defect in H3-K56ac of ΔAsf1 yeast*

Asf1^{Sc} and the fungal-specific HAT Rtt109 collaborate to acetylate histone H3 at K56 [18–20]. We asked whether Asf1^{Tt} could functionally complement budding yeast deleted for Asf1. We used a CEN-based plasmid system to express epitope tagged full length *ASF1^{Tt}* or *ASF1^{Sc}* in Δ*asf1* budding yeast cells that exhibit a slow growth phenotype. Compared to *ASF1^{Sc}*, expression of *ASF1^{Tt}* did not complement the slow growth phenotype of the Δ*asf1* mutant (Fig. 6A). The slow growth of Δ*asf1* strains in yeast is due to lack of H3K56ac [21]. H3K56ac is an abundant modification in *Tetrahymena* MAC [39]. Although *Asf1^{Tt}* was expressed at the same level as *ASF1^{Sc}* as judged by Western blotting, it did not rescue the H3K56 acetylation defect in the budding yeast (Fig. 6B). Similarly, when expressed

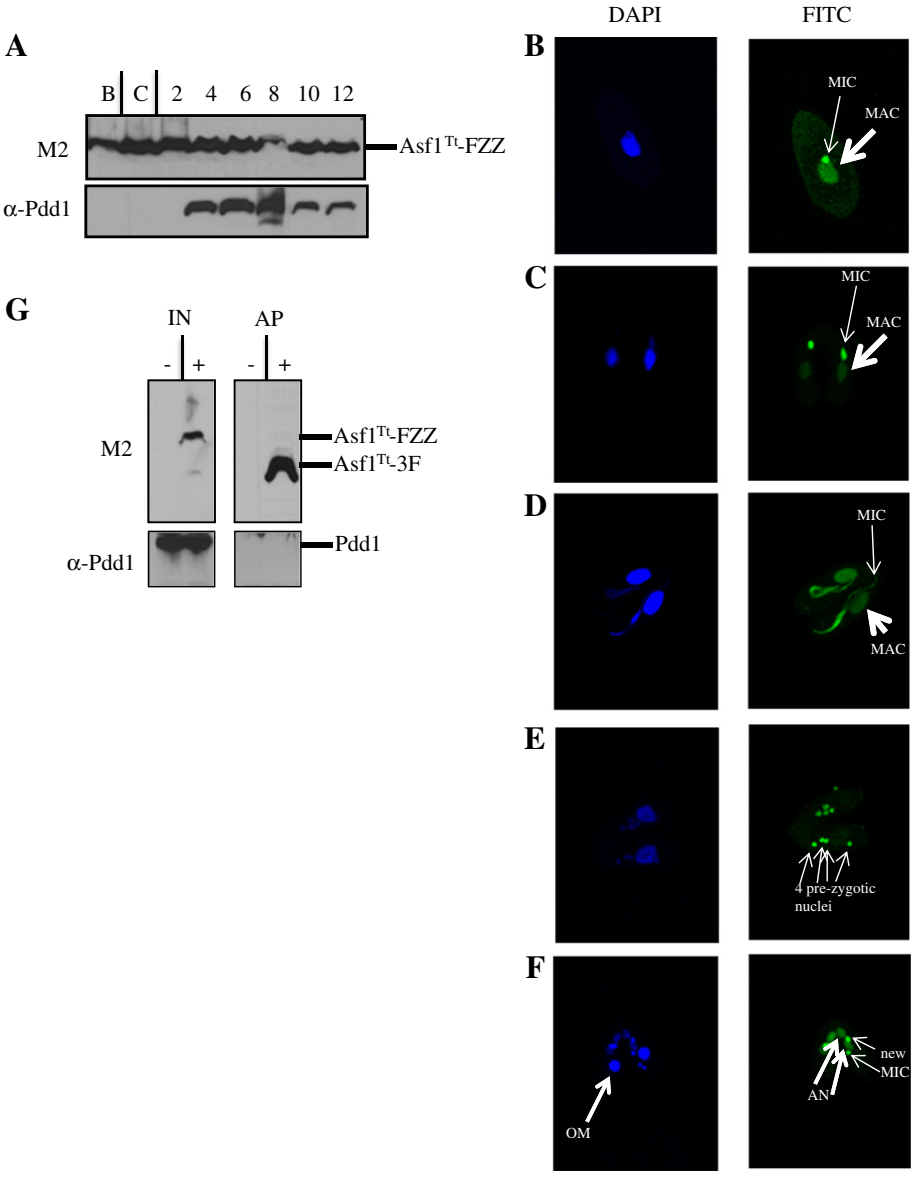

Fig. 4 – Analysis of Asf1-FZZ from conjugating cells. A: Western blot analysis of whole cell extracts from indicated times post-mixing of B2086 and Cu428 strains both expressing Asf1^{Tt}-FZZ from their MAC. B–F: Indirect immunofluorescence using M2 antibody of starved (C) or conjugating (D–G) B2086 and Cu428 strains both expressing Asf1^{Tt}-FZZ from their MAC. G: Western blot analysis of tandem affinity purified Asf1^{Tt}-FZZ (lane "+") from the conjugation of B2086 and Cu428 strains both expressing Asf1^{Tt}-FZZ from their MAC harvested at 6 h post-mixing. Mock AP was performed from a mating of untagged B2086 and Cu428 (lane "–").

as a recombinant protein, Asf1^{Tt} did not synergize with recombinant Rtt109 in vitro, as did Asf1^{Sc} (Fig. 6C). In human cells Gcn5^{Hs} has been reported to acetylate H3K56 [23]. We did not observe H3K56ac in vitro using recombinant *T. thermophila* Gcn5/p55 either alone, or in combination with Asf1^{Sc} or Asf1^{Tt} (Fig. 6C). To address whether Asf1 is required in vivo for H3K56ac in *T. thermophila* we attempted to generate a somatic knockout by integrating a neomycin resistance cassette in place of the *ASF1*^{Tt} coding region at its MAC locus (Supplemental Fig. 5A). If a gene is non-essential for growth in *T. thermophila*, it should be possible to replace all MAC copies by using an increasing concentration of the selective drug paromomycin in phenotypic assortment. We were not able to replace all MAC copies using phenotypic assortment, indicating that the *ASF1* gene is required for growth of *T. thermophila* (Supplemental Fig. 5B). 'Knock-down' cells partially assorted for the knockout construct did not show reduced levels of H3K56ac (Supplemental Fig. 5C).

2.7. *Gene network analysis of ASF1^{Tt} and IMPB6*

We used publicly available gene expression data [58] to compare gene expression profiles of *ASF1*^{Tt} with those of the genes encoding its co-purifying proteins. Hierarchical

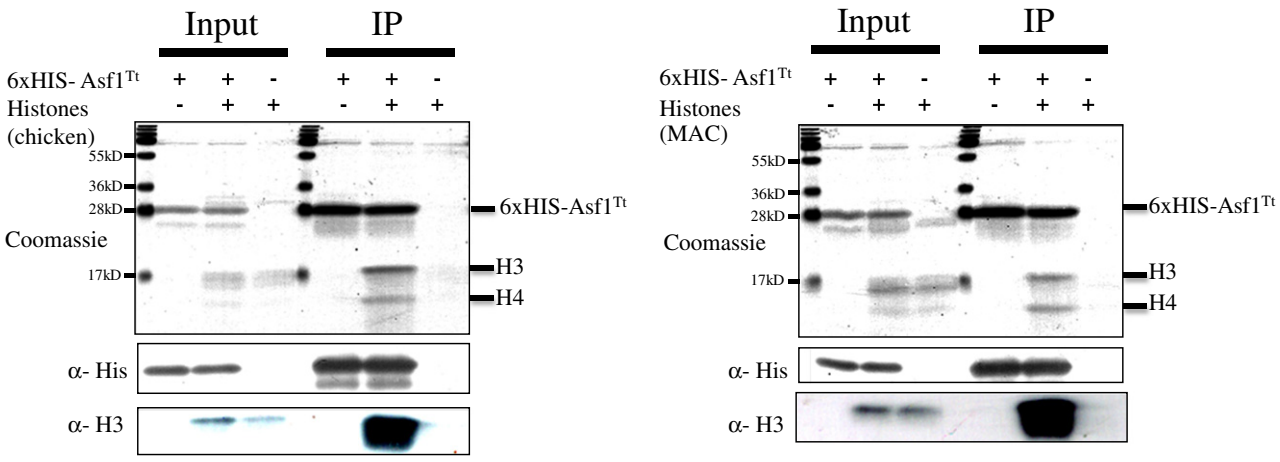

Fig. 5 – Recombinant Asf1^{Tt} binds histones H3 and H4. Pull-down reactions were separated by electrophoresis through 15% SDS-PAGE and stained with Coomassie blue or immunoblotted with the indicated antibodies.

clustering was used to compare the patterns by similarities in their gene expression profiles (Fig. 7A). This analysis revealed that within this group, *ASF1* and *IMPB6* cluster together due to their very similar gene expression profiles, consistent with their apparent functional linkage. Similarities in *T. thermophila* gene expression profiles have been used to construct gene networks which allow predictions about gene functioning in particular pathways, or as part of the same protein complex [58,59] (http://tfgd.ihb.ac.cn/). Since *ASF1*^{Tt} and *IMPB6* have similar patterns of gene expression (Fig. 7A), co-purify (Fig. 2G, Table 1), and have very similar localization patterns in growing cells (Fig. 3A), we used the publicly available microarray data to construct such a gene network and extracted the subnetwork for the genes encoding Asf1^{Tt}, *IMPB6*, *NRP1*, and their first neighbors (Fig. 7B) to identify genes that may function in the same pathway (Fig. 7C). We included *NRP1* in this analysis since its encoded protein's physical interaction with Asf1^{Tt} is evolutionarily conserved among most eukaryotes. The subnetwork includes 230 genes and 3694 links between them (Supplemental data 1–3). *ASF1*, *IMPB6*, *NRP1* and their first neighbors form a connected component (Fig. 7B). We identified 130 genes in the subnetwork specifically linked to *ASF1*^{Tt}, 61 to *IMPB6*, and 62 to *NRP1* (Fig. 7C). Interestingly, *ASF1* and *IMPB6* share 40 neighboring genes including themselves, (Supplemental Fig. 6), a set of genes including one that encodes MicNup98A/TTHERM_01080600 and MicNup98B/TTHERM_00530720 whose function is to block the entry of MAC proteins into the MIC [60], as well as putative CAF-1 subunit *CAC2* (TTHERM_00219420), and putative members of FACT^{Tt}, *POB3* (TTHERM_00049080) and *CET1/SPT16* (TTHERM_00283330) (Supplemental Table 3). In addition, *HIR1*^{Tt} (TTHERM_00046490), another putative histone chaperone, is linked to *ASF1*^{Tt} (Supplementary Table 3). *ASF1*^{Tt} and *NRP1* have 11 nodes in common while *NRP1* and *IMPB6* overlap by three (Fig. 7C). TTHERM_00048980 which encodes putative leading strand DNA polymerase subunit *DPB2*^{Tt} is linked to *ASF1*^{Tt}, *IMPB6* and *NRP1* (Fig. 7C, Supplemental Table 3), consistent with a role for these three functions in coordinating proper flow of replication dependent histones H3 and H4.

3. Discussion

Asf1 is highly conserved throughout eukaryotes, found even in highly diverged eukaryotes such as *Guillardia theta* and *Giardia lamblia* [41,61] and likely was encoded in the last common ancestor of eukaryotes [62]. Most molecular analysis of Asf1 has been performed using human or yeast models but information on the role of Asf1 in eukaryotes outside the Opisthokonta remains limited. To address this we have initiated proteomic analysis of *T. thermophila* Asf1. The statistical analysis of our AP–MS data set of Asf1^{Tt}-interacting proteins showed that it co-purifies with a set of proteins in vegetative growth and development that includes an importin β, ImpB6, in addition to Nrp1, a protein similar to human NASP. These Asf1 interaction partners are also found in budding yeast and human cells. In addition, multiple connections exist between the genes encoding these proteins in our network analysis of gene expression data. Thus as well as being a conserved H3–H4 binding protein, its protein–protein interactions with Importin β and NASP are also conserved through different branches of eukaryotes from *T. thermophila* (Alveolata) to fungi to animals (both Opisthokonta). Analogous to what has been proposed for humans and yeast [30,63], we suggest that Asf1–ImpB6 function together to transport newly synthesized H3–H4 into both the MIC and MAC (Fig. 8). Interestingly, when we assessed ImpB6 protein–protein interactions, we found Aip1 and a BRCT domain protein as major interacting proteins as assessed by SAINT analysis, as well as Aip2, and Asf1^{Tt} suggesting that the major function of ImpB6, one of eleven importin β's encoded by *T. thermophila* [55], is the regulation of transport of histones H3 and H4 into the MAC and MIC via Asf1^{Tt} and possibly Aip1 and Aip2. ImpB6 may form multiple sub-complexes which, despite an efficient purification of ImpB6, may lead to purifying many of its interaction partners at a concentration close or below our limit of detection. In humans, NASP is believed to function upstream of Asf1 in the cytoplasm, binding Hat1–RbAp46 which acetylates newly

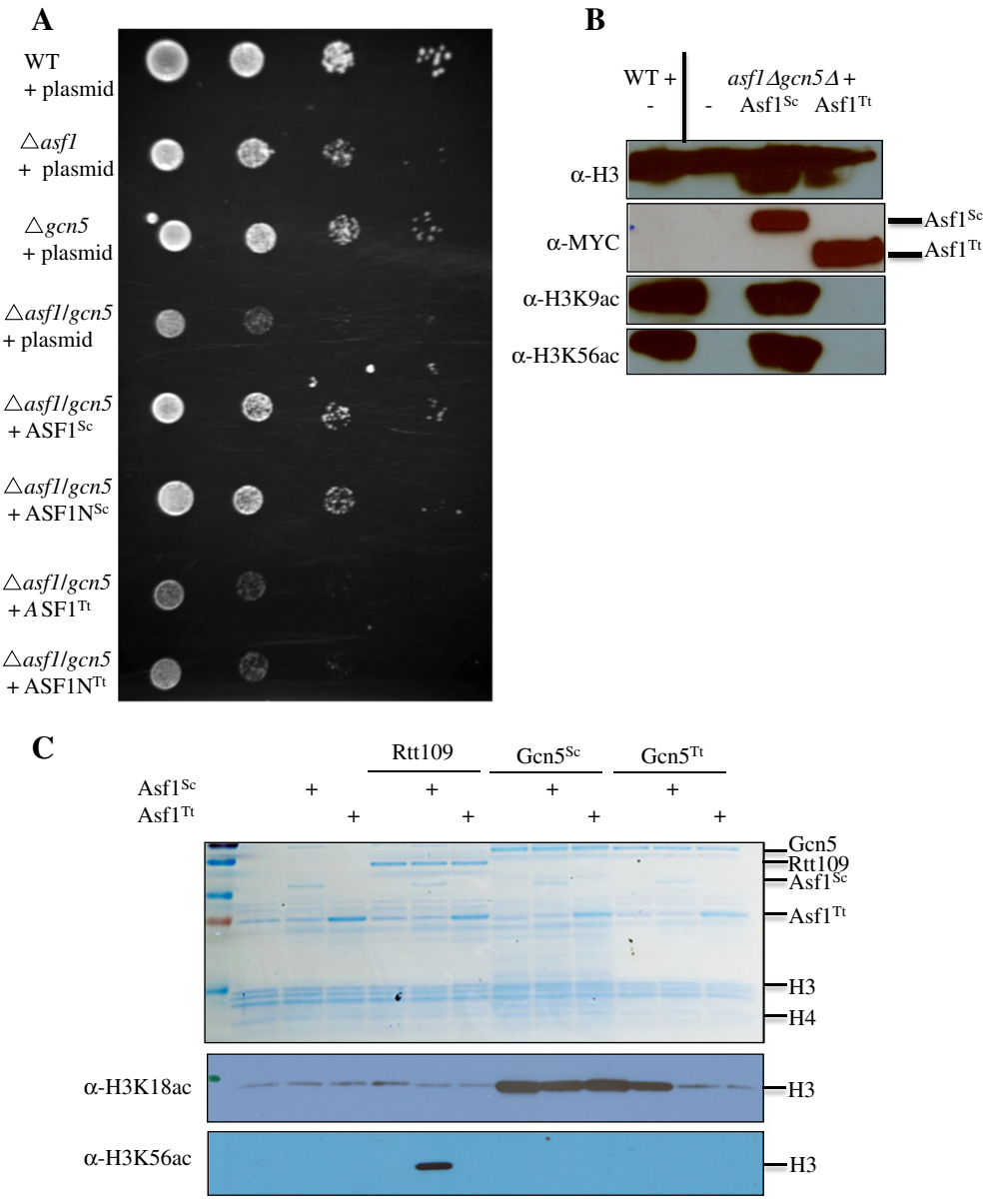

Fig. 6 – Asf1^{Tt} does not synergize with the fungal HAT Rtt109. A: Dilutions of indicated *S. cerevisiae* strains were spotted on —LEU media and grown 2–3 days. B: WCE of indicated strains were separated by electrophoresis through 15% SDS-PAGE and blotted with the indicated antibodies. C: Individual histone acetyltransferase assays were performed using the indicated recombinant proteins and separated by electrophoresis through 15% SDS-PAGE which were immunoblotted using antibodies indicated or stained with Coomassie blue.

translated histone H4 at K5 and K12 before passing it to Asf1 [30]. Asf1 also interacts with the NASP-family member Hif1 in yeast [27,64]. Further work will be required to determine whether, similar to human cells, Nrp1 transfers histones to Asf1^{Tt} in the cytoplasm (Fig. 8) or accepts them from Asf1 in the MAC and/or MIC. Proteomic analysis of H3.1 and H3.3 interacting proteins (Fillingham et al., unpublished observations) should help to resolve this question.

Since the MAC and MIC exhibit different chromatin structures and timing of DNA replication, it will be of interest to determine the identity of nucleus-specific elements to chromatin assembly pathways. Our network analysis which showed no connectivity between *ASF1*^{Tt} and *AIP1*, *AIP2* and *AIP3* is consistent with functional roles outside of Asf1–ImpB6–Nrp1 control of nuclear transport of histones H3 and H4. Additional evidence for roles outside of nuclear transport for Asf1^{Tt} includes the fact that Aip3 localizes exclusively to the MIC (Fig. 3D). In addition, its expression pattern differs from that of *ASF1*^{Tt} and *IMPB6* (Fig. 7A). The Aip3 protein consists of an N-terminal RING domain, followed by a C-terminal tandem BRCT domain. Our bioinformatic analysis of AIP3 tandem BRCT domain

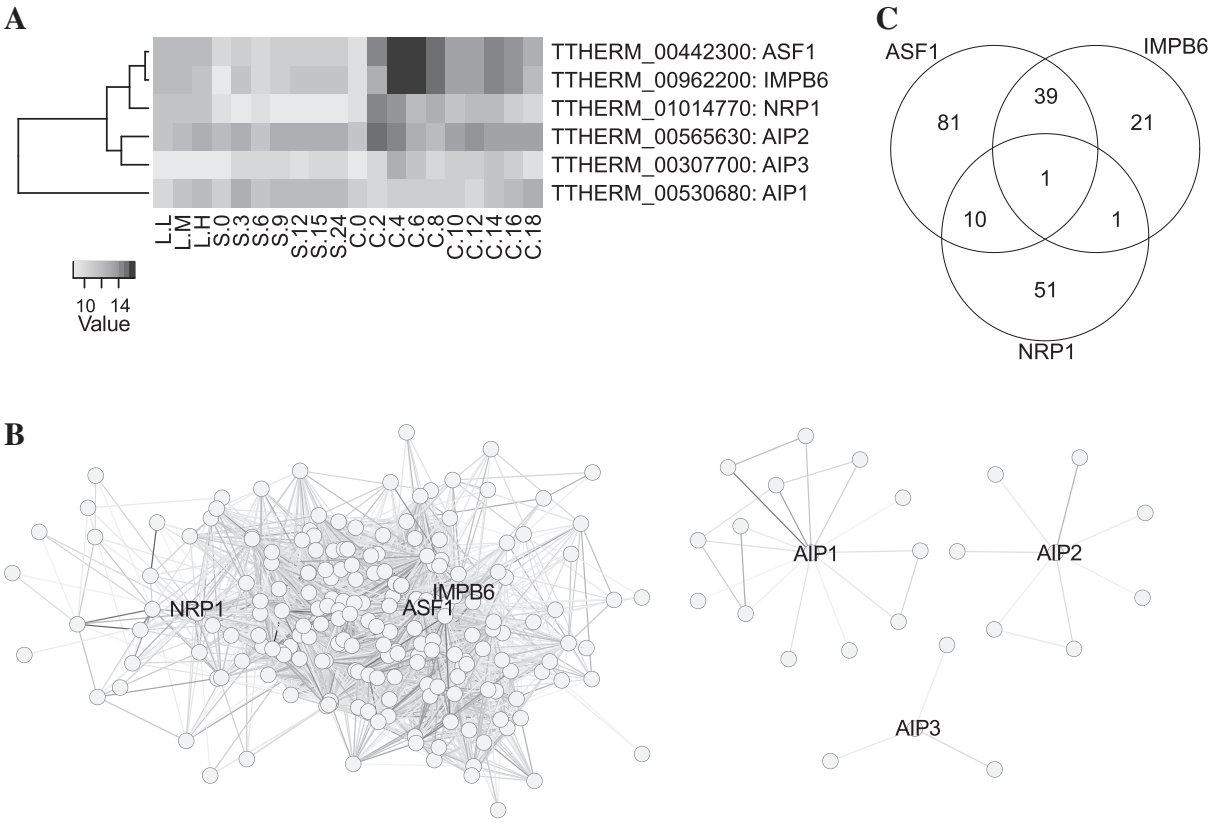

Fig. 7 – Gene expression network analysis of *ASF1*^{Tt}. A. Hierarchal clustering of gene expression data of Asf1^{Tt} and genes encoding its co-purifying proteins. B. Subnetwork for the genes encoding *ASF1*^{Tt}, *IMPB6*, *NRP1*, *AIP1*, *AIP2*, *AIP3* and their first neighbors. *Asf1*^{Tt}, *IMPB6* and *NRP1* form a connected component. C. Venn diagram representation of the *Asf1*^{Tt}, *IMPB6*, and *NRP1* components.

indicates similarity to that of Rtt107 and Mdc1 of yeast/human cells, both of which have been shown to bind the phosphorylated serine residue of the γH2AX modification [65,66]. The γH2A modification in *T. thermophila* is MIC-specific [67] as is Aip3 (Fig. 3D). The RING domain is found in proteins that function in protein ubiquitination pathways. Further work is required to determine whether Asf1^{Tt}-mediated chromatin assembly/disassembly is connected to γH2AX and/or protein ubiquitination. The Aip1 and Aip2 that co-purify with both Asf1^{Tt}-FZZ and ImpB6-FZZ are additional candidates for nuclear specific roles. Although no significant sequence similarity exists between Aip1, Aip2 and human Codanin, it is tempting to predict that similar to human cells there exists a regulation at the level of nuclear import. Towards this end it will be informative to examine phenotypes of epitope tagged and knock-outs of *AIP1* and *AIP2*.

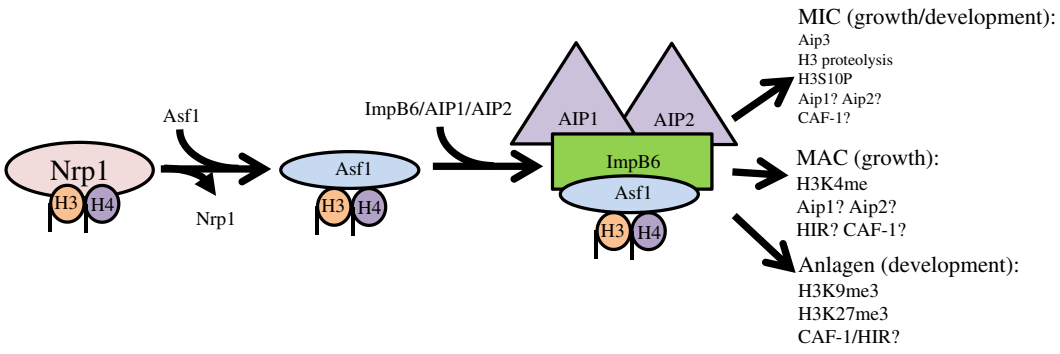

Fig. 8 – Model for Asf1 function in the MAC and MIC of *T. thermophila*. See text for details.

In humans and yeast Asf1 has been demonstrated to function upstream of RI and RD chromatin assembly via mutually exclusive direct physical interactions with either of two WD40 repeat proteins, Cac2p and HirA (Hir1p and Hir2p in *S. cerevisiae*) of the CAF and HIR histone chaperone complexes. The direct physical interaction is mediated by the β4–β5 region of Asf1 and a short, conserved sequence called the B domain in Cac2/HIRA (Hir1 in Sc). Our comparative sequence analysis indicates possible differences in this region in $Asf1^{Tt}$, and our analysis of Asf1 interacting proteins in growing cells revealed no peptides from putative *T. thermophila* HIR or CAF-1 subunits. However, since our network analysis of *T. thermophila* expression data shows clustering of Asf1 and *IMPB6* with genes encoding putative HIRA and CAF-1 subunits (Fig. 7C, Supplemental Table 3), we predict that $Asf1^{Tt}$ does function upstream of chromatin assembly in the MAC and MIC. Interestingly $Hira^{Tt}$ (TTHERM_00046490) but none of the predicted $Caf\text{-}1^{Tt}$ subunits contains the canonical B domain (data not shown). Further work will be required to determine the nature of the physical interactions/histone transfer of $Asf1^{Tt}$ with $Hira^{Tt}$ or $Caf\text{-}1^{Tt}$.

As expected from the high degree of sequence conservation, $Asf1^{Tt}$ binds histones H3 and H4 in vitro. However $Asf1^{Tt}$ cannot functionally complement $Asf1^{Sc}$ in vivo or in vitro in its role in Rtt109-based H3K56ac. This lack of synergy between $Asf1^{Tt}$ and Rtt109 suggests there are differences in Asf1 orthologues among eukaryotes [4,68]. It has been suggested that when $Asf1^{Sc}$ binds H3 and H4 it makes H3K56 more accessible to Rtt109 [45]. Our results suggest that there may be subtle but significant differences in the way different Asf1 proteins bind the H3–H4 dimer. Structural studies of $Asf1^{Tt}$ will help resolve this question. This and the fact that our Asf1 knock-down did not alter levels of H3K56ac indicate that in *T. thermophila* Asf1 is not required for H3K56ac, although conclusive proof must await the analysis of a germ-line Asf1 knockout.

T. thermophila has abundant H3K56ac [39] but does not appear to encode recognizable versions of the fungal or mammalian H3K56-specific HATs RTT109 or CBP/p300. $Gcn5^{Tt}$ does not possess H3K56ac activity. The evolutionary divergence of fungal Rtt109 as well as the importance of the H3K56ac pathway to fungal viability present a possible target for the design of novel anti-fungal pharmaceuticals [69]. It will be informative to determine if there exists a novel H3K56-specific HAT in *T. thermophila* which is relatively closely related to several medically relevant Apicomplexa which includes the *Plasmodium* species that cause malaria [70].

4. Materials and methods

4.1. Cell strains

T. thermophila strains CU428 [*Mpr/Mpr* (VII, mp-s)] and B2086 [Mpr^{+}/Mpr^{+} (II, mp-s)] of inbreeding line B were obtained from the *Tetrahymena* Stock Center, Cornell University, Ithaca N.Y. (http://tetrahymena.vet.cornell.edu/). Cells were cultured axenically in 1× SPP at 30 °C as previously described [71]. The strains of *S. cerevisiae* used in this study are shown in Table S1.

4.2. Protein expression

Full-length Rtt109, $Asf1^{Sc}$, $Asf1^{Tt}$, $Gcn5^{Sc}$ and $Gcn5^{Tt}$ were cloned into pET14b or pET28a. Recombinant proteins were expressed and purified as in [27].

4.3. Sequence alignments

Multiple sequence alignments of Asf1 amino acid sequence from various model organisms were performed using ClustalW (http://bioweb.pasteur.fr/seqanal/interfaces/clustalw.html#profile) and then shaded by importing the ALN file into the Boxshade server (http://www.ch.embnet.org/software/BOX_form.html).

4.4. Oligonucleotides

See Table S2 for a list of the oligonucleotides used during the course of this study.

4.5. Affinity purification

Frozen cell pellets from ~500 ml of growing *T. thermophila* harvested at 3×10^5 cells/ml were used. The pellets were thawed and re-suspended in 10 mM Tris–HCl (pH 7.5), 1 mM $MgCl_2$, 300 mM NaCl and 0.2% NP40 plus yeast protease inhibitors (Sigma). 500 units of Benzonase nuclease (Sigma E8263) were added and extracts were incubated for 30 min at 4 °C. WCEs were clarified by centrifugation at 16,000 ×*g* with soluble material incubated for 4 h in the presence of 200 μl IgG Sepharose (Amersham). The IgG-Sepharose was washed once with 10 ml IPP300 (10 mM Tris–HCl pH 8.0, 300 mM NaCl, 0.1% NP40) and three times with 10 ml TEV100 buffer (10 mM Tris–HCl pH 8.0, 100 mM NaCl, 0.1% NP40, 1 mM EDTA) before being treated overnight with TEV protease as described [72]. The soluble extract was then added to 30 μl of packed M2-agarose (Sigma) and incubated at 4 °C for 2 h. The M2-agarose was subsequently washed four times with 750 μl of IP100 buffer (10 mM Tris–HCl pH 8.0, 100 mM NaCl). Elution was performed with either 3xFLAG peptide (100 μg/ml) or 0.5 M NH_4OH.

4.6. Tryptic digestion and mass spectrometry analysis

TAP purified proteins eluted in 0.5 M NH_4OH were taken to dryness in a speed-vac without heat. The proteins were digested with trypsin in a solution as previously described ([73]; alternate protocol 1). The resulting peptides were manually bomb loaded onto a capillary column (75 μm id), packed in-house with 10 cm Reprosil-Pur 120 C18-AQ, 3uM (Dr-Maisch GmbH; Germany), pre-equilibrated with 2% acetonitrile (ACN), 0.1% formic acid. The column was placed in-line with an LTQ mass spectrometer equipped with an Agilent 1100 capillary HPLC delivering 200 nl/min using a split flow arrangement. Buffer A was 2% ACN and 0.1% formic acid; buffer B was 98% ACN and 0.1% formic acid. The HPLC gradient program delivered an ACN gradient over 120 min (1–5% buffer B over 4 min, 5–40% buffer B over 100 min, 40–60% buffer B over 5 min, 60–100% buffer B over 5 min, hold buffer B at 100% 3 min and 100–0% B in 2 min). The parameters for data dependent acquisition on the mass spectrometer were: 1 centroid MS (mass

range 400–2000) followed by MS/MS on the 5 most abundant ions. General parameters were: activation type = CID, isolation width = 3, normalized collision energy = 32, activation Q = 0.25, activation time = 30 ms, wideband activation. For data dependent acquisition, minimum threshold was 1000, the repeat count = 1, repeat duration = 30 s, exclusion size list = 500, exclusion duration = 30 s, exclusion mass width (by mass) = low 1.2, high 1.5. The resulting RAW files were saved on a local interaction proteomics LIMS, ProHits [74] and mgf files were generated using the ProteoWizard converter implemented within ProHits (–filter 'peakPicking true2'–filter 'msLevel2'). The mzXML files were searched with Mascot version 2.3 against the RefSeq *T. thermophila* protein database (V45 containing 24,770 sequences; released on January 24th 2011), allowing for one missed cleavage site and methionine oxidation as a variable modification. The fragment mass tolerance was 0.6 Da (monoisotopic mass) and the mass window for the precursor was +/−3 Da average mass. An ion score cutoff of 35 was selected and a protein hit required at least two "bold red peptides" to be considered. To identify significant interaction partners from the affinity purification data, the data were subjected to SAINTexpress analysis [51,52] using SAINTexpress (v3.03), a new implementation of the model-based scoring algorithm with improved computational efficiency and enhanced stability in parameter estimation (Teo et al., submitted). The average SAINT scores were calculated for the best two experimental samples for each bait analyzed (compress baits to 2). When >4 negative controls were available, the 4 maximal spectral counts for each prey were used for modeling (compress controls to 4).

4.7. Histone binding assay

In vitro histone binding was done using chicken erythrocyte histones (Millipore) or *T. thermophila* macronuclear total acid soluble histones extracted from starved *T. thermophila* as described previously [75]. Both full-length and 1–155 versions of recombinant 6xHIS-Asf1^{Tt} were incubated with a histone mixture in buffer (50 mM Tris–HCl (pH 7.5), 500 mM NaCl, 5 mM $MgCl_2$, 1 mM dithiothreitol, 0.5 mM phenylmethylsulfonyl fluoride and 1 mM benzamidine). Approximately 50 μg of either chicken erythrocyte or *T. thermophila* MAC histone mixture were added along with 100 μg of recombinant Asf1 to a total of 750 μl. The mixture was rotated at 30 °C for 30 min. Fifty microliters was obtained for input and 20 μl of packed nickel beads was added to the remaining mixture followed by a 15 min rotation at 4 °C to recover the HIS-tagged enzymes and any associated histone. Next, the beads were washed four times with the assay buffer. The sample was eluted by boiling the beads in SDS loading buffer supplemented with 0.1 M EDTA. The eluate was electrophoresed through 15% SDS-PAGE and stained with Coomassie blue, or transferred to nitrocellulose for Western blots as needed.

4.8. HAT assays

HAT assays were performed as described [27] using as substrate chicken core histones (Millipore). HAT assays were incubated for 45 min at 30 °C in a 30 μl volume containing 5 μg core histones total substrate, 50 mM Tris–HCl (pH 8.0), 50 mM NaCl, 5 mM $MgCl_2$, 1 mM dithiothreitol, 3.3 nCi [^{14}C]acetyl-CoA (60 mCi/mmol), and 1 mM phenylmethylsulfonyl fluoride. Five microliter aliquots of recombinant proteins (adjusted to 0.5 μg/μl) were added to each reaction. Reactions were stopped by the addition of 30 μl 2× sodium dodecyl sulfate-polyacrylamide gel electrophoresis (SDS-PAGE) loading dye and boiled. Aliquots (20% of total volume) were electrophoresed in parallel through several 15% SDS-PAGE gels. One gel was fixed and stained with Coomassie blue, saturated with Enlightning (Perkin Elmer), dried under vacuum, and either exposed to film or imaged using a Typhoon phosphorimager. Other gels were treated with gel code blue (Fisher Scientific) or transferred to nitrocellulose for Western blot analysis.

4.9. Generation of WCE and Western blotting

S. cerevisiae whole-cell extracts (WCE) were generated using trichloroacetic acid and glass beads as described [27]. WCEs were separated by electrophoresis through 15% SDS-PAGE, transferred to nitrocellulose, and blotted with the indicated antibodies. Antibodies and dilutions used were anti-H3 (1:2000; Abcam), anti-H3-K9ac (1:10,000; Abcam), anti-H3-K56ac (1:5000; Upstate), anti-H3-K18ac (1:15,000; Lake Placid Biologicals), and anti-Pdd1 (1:3000 Abcam).

4.10. DNA manipulations

Whole-cell DNA was isolated from *T. thermophila* strains as described [76]. Molecular biology techniques were carried out using standard protocols or by following a supplier's instructions. The double-stranded DNA probes for Northern and Southern analysis were labeled by random priming with [α-^{32}P]dATP (Amersham). DNA-modifying enzymes were obtained from New England Biolabs. Southern blots were imaged and quantified with a Canberra Packard Instant Imager.

4.11. Macronuclear gene replacement

Epitope tagging vectors for Asf1^{Tt}, ImpB6 and NASP^{Tt} were constructed by amplifying two separate ~1 kb fragments up and downstream of its stop codon using WT *T. thermophila* genomic DNA as template using primers as outlined in Table S2. Upstream and downstream PCR products were digested either with *KpnI* and *SacI* or *NotI* and *SacII* before being cloned into the appropriate sites within the tagging vector provided by Dr. Kathleen Collins (University of California, Berkeley, CA). The resulting plasmid was digested with *KpnI* and *SacII* prior to transformation. One micrometer gold particles (60 mg/ml; Bio-Rad) were coated with 5 μg of the digested plasmid and introduced into the *Tetrahymena* macronucleus using biolistic transformation with a PDS-1000/He Biolistic particle delivery system (Bio-Rad). Transformants were identified by growth to saturation in a paromomycin concentration of 60 μg/ml. Transformants were grown in increasing concentrations of paromomycin to a final concentration of 1 mg/ml.

4.12. Indirect immunofluorescence

The cells were harvested and fixed for indirect immunofluorescence [77] using the method of Wenkert and Allis [78]. Incubation of fixed cells dried on coverslips with primary

mouse M2 (Sigma) or anti-GFP (Roche) antisera was at a 1:200 dilution at 4 °C overnight. Secondary antibody was fluoresced in isothiocyanate-conjugated goat anti-mouse (Pierce) for 1 h at room temperature. Nuclear counterstaining was with 4,6-diamidino-2-phenylindole dihydrochloride for confocal microscopy using an Olympus BX51 fluorescence microscope.

4.13. *Gene expression analysis*

Microarray expression data set with accession number GSE11300 was downloaded from Gene Expression Omnibus (GEO). This data set includes a total of 50 NimbleGene microarrays spanning the entire life cycle of *T. thermophila*. Background subtraction, quantile normalization and summarization via median polish were performed using the RMA algorithm as implemented in the package affy (affy_1.32.1) [79] for R. Replicates were averaged and the resulting expression values, on the $\log_2$ scale, were used to construct a gene expression network with the unsupervised method Context Likelihood of Relatedness (CLR) [80]. The Matlab implementation of the algorithm CLRv1.2.2 was used. The network was cut at a Z-score threshold of 4.54 (FDR = 0.1), leaving 25,672 genes and 234,561 links between them. The orthology database OrthoMCL [54] (release 5) containing ortholog groups of protein sequences of 150 genomes was downloaded. Ortholog groups and protein domains were used as additional annotation to the nodes in the network to help identify genes of interest based on their similarity to genes in other species or their domain architecture.

Supplementary data to this article can be found online at http://dx.doi.org/10.1016/j.jprot.2013.09.018.

Funding

This work was supported by: NSERC Discovery Grants to J.S.F. (grant number: 386646-2010) and R.E.P. (grant number: 539509), Ryerson University Health Sciences Fund (J.S.F.), and operating grants from CIHR to R.E.P. (grant number: MOP13347), and A.-C.G. and T.P. (grant number: MOP 123322). A.-C.G. holds a Canada Research Chair in Functional Proteomics and the Lea Reichmann Chair in Cancer Proteomics. J.-P.L. is supported by postdoctoral awards from the Canadian Institutes of Health Research and the Natural Science and Engineering Research Council.

Acknowledgments

We thank Dr. Judith Recht for the critical reading of this manuscript. We also thank Guo Ci Teo and Hyungwon Choi (National University of Singapore) for providing early access to SAINTexpress, and Guomin Liu for the implementation of the SAINTexpress algorithm within ProHits.

REFERENCES

[1] Alabert C, Groth A. Chromatin replication and epigenome maintenance. Nat Rev Mol Cell Biol 2012;13:153–67.
[2] De Koning L, Corpet A, Haber JE, Almouzni G. Histone chaperones: an escort network regulating histone traffic. Nat Struct Mol Biol 2007;14:997–1007.
[3] Corpet A, De Koning L, Toedling J, Savignoni A, Berger F, Lemaitre C, et al. Asf1b, the necessary Asf1 isoform for proliferation, is predictive of outcome in breast cancer. EMBO J 2011;30:480–93.
[4] Das C, Lucia MS, Hansen KC, Tyler JK. CBP/p300-mediated acetylation of histone H3 on lysine 56. Nature 2009;459:113–7.
[5] Ask K, Jasencakova Z, Menard P, Feng Y, Almouzni G, Groth A. Codanin-1, mutated in the anaemic disease CDAI, regulates Asf1 function in S-phase histone supply. EMBO J 2012;31:2013–23.
[6] Elsasser SJ, Allis CD, Lewis PW. Cancer. New epigenetic drivers of cancers. Science 2011;331:1145–6.
[7] Alekseev OM, Richardson RT, Tsuruta JK, O'Rand MG. Depletion of the histone chaperone tNASP inhibits proliferation and induces apoptosis in prostate cancer PC-3 cells. Reprod Biol Endocrinol 2011;9:50.
[8] Schwartzentruber J, Korshunov A, Liu XY, Jones DT, Pfaff E, Jacob K, et al. Driver mutations in histone H3.3 and chromatin remodelling genes in paediatric glioblastoma. Nature 2012;482:226–31.
[9] Chan KM, Fang D, Gan H, Hashizume R, Yu C, Schroeder M, et al. The histone H3.3K27M mutation in pediatric glioma reprograms H3K27 methylation and gene expression. Genes Dev 2013;27:985–90.
[10] Le S, Davis C, Konopka JB, Sternglanz R. Two new S-phase-specific genes from *Saccharomyces cerevisiae*. Yeast 1997;13:1029–42.
[11] Tyler JK, Adams CR, Chen SR, Kobayashi R, Kamakaka RT, Kadonaga JT. The RCAF complex mediates chromatin assembly during DNA replication and repair. Nature 1999;402:555–60.
[12] Adkins MW, Howar SR, Tyler JK. Chromatin disassembly mediated by the histone chaperone Asf1 is essential for transcriptional activation of the yeast PHO5 and PHO8 genes. Mol Cell 2004;14:657–66.
[13] Fillingham J, Kainth P, Lambert JP, van Bakel H, Tsui K, Pena-Castillo L, et al. Two-color cell array screen reveals interdependent roles for histone chaperones and a chromatin boundary regulator in histone gene repression. Mol Cell 2009;35:340–51.
[14] Prado F, Cortes-Ledesma F, Aguilera A. The absence of the yeast chromatin assembly factor Asf1 increases genomic instability and sister chromatid exchange. EMBO Rep 2004;5:497–502.
[15] Schulz LL, Tyler JK. The histone chaperone Asf1 localizes to active DNA replication forks to mediate efficient DNA replication. FASEB J 2006;20:488–90.
[16] Ramey CJ, Howar S, Adkins M, Linger J, Spicer J, Tyler JK. Activation of the DNA damage checkpoint in yeast lacking the histone chaperone anti-silencing function 1. Mol Cell Biol 2004;24:10313–27.
[17] Feser J, Truong D, Das C, Carson JJ, Kieft J, Harkness T, et al. Elevated histone expression promotes life span extension. Mol Cell 2010;39:724–35.
[18] Han J, Zhou H, Horazdovsky B, Zhang K, Xu RM, Zhang Z. Rtt109 acetylates histone H3 lysine 56 and functions in DNA replication. Science 2007;315:653–5.
[19] Driscoll R, Hudson A, Jackson SP. Yeast Rtt109 promotes genome stability by acetylating histone H3 on lysine 56. Science 2007;315:649–52.
[20] Collins SR, Miller KM, Maas NL, Roguev A, Fillingham J, Chu CS, et al. Functional dissection of protein complexes involved in yeast chromosome biology using a genetic interaction map. Nature 2007;446:806–10.
[21] Recht J, Tsubota T, Tanny JC, Diaz RL, Berger JM, Zhang X, et al. Histone chaperone Asf1 is required for histone H3 lysine

56 acetylation, a modification associated with S phase in mitosis and meiosis. Proc Natl Acad Sci U S A 2006;103:6988–93.
[22] Vempati RK, Jayani RS, Notani D, Sengupta A, Galande S, Haldar D. p300-mediated acetylation of histone H3 lysine 56 functions in DNA damage response in mammals. J Biol Chem 2010;285:28553–64.
[23] Tjeertes JV, Miller KM, Jackson SP. Screen for DNA-damage-responsive histone modifications identifies H3K9Ac and H3K56Ac in human cells. EMBO J 2009;28:1878–89.
[24] Emili A, Schieltz DM, Yates III JR, Hartwell LH. Dynamic interaction of DNA damage checkpoint protein Rad53 with chromatin assembly factor Asf1. Mol Cell 2001;7:13–20.
[25] Green EM, Antczak AJ, Bailey AO, Franco AA, Wu KJ, Yates III JR, et al. Replication-independent histone deposition by the HIR complex and Asf1. Curr Biol 2005;15:2044–9.
[26] Prochasson P, Florens L, Swanson SK, Washburn MP, Workman JL. The HIR corepressor complex binds to nucleosomes generating a distinct protein/DNA complex resistant to remodeling by SWI/SNF. Genes Dev 2005;19:2534–9.
[27] Fillingham J, Recht J, Silva AC, Suter B, Emili A, Stagljar I, et al. Chaperone control of the activity and specificity of the histone H3 acetyltransferase Rtt109. Mol Cell Biol 2008;28:4342–53.
[28] Groth A, Corpet A, Cook AJ, Roche D, Bartek J, Lukas J, et al. Regulation of replication fork progression through histone supply and demand. Science 2007;318:1928–31.
[29] Tagami H, Ray-Gallet D, Almouzni G, Nakatani Y. Histone H3.1 and H3.3 complexes mediate nucleosome assembly pathways dependent or independent of DNA synthesis. Cell 2004;116:51–61.
[30] Campos EI, Fillingham J, Li G, Zheng H, Voigt P, Kuo WH, et al. The program for processing newly synthesized histones H3.1 and H4. Nat Struct Mol Biol 2010;17:1343–51.
[31] Alvarez F, Munoz F, Schilcher P, Imhof A, Almouzni G, Loyola A. Sequential establishment of marks on soluble histones H3 and H4. J Biol Chem 2011;286:17714–21.
[32] Zhang H, Han J, Kang B, Burgess R, Zhang Z. Human histone acetyltransferase 1 protein preferentially acetylates H4 histone molecules in H3.1–H4 over H3.3–H4. J Biol Chem 2012;287:6573–81.
[33] Lamour V, Lecluse Y, Desmaze C, Spector M, Bodescot M, Aurias A, et al. A human homolog of the *S. cerevisiae* HIR1 and HIR2 transcriptional repressors cloned from the DiGeorge syndrome critical region. Hum Mol Genet 1995;4:791–9.
[34] Elsaesser SJ, Allis CD. HIRA and Daxx constitute two independent histone H3.3-containing predeposition complexes. Cold Spring Harb Symp Quant Biol 2010;75:27–34.
[35] Ridgway P, Almouzni G. CAF-1 and the inheritance of chromatin states: at the crossroads of DNA replication and repair. J Cell Sci 2000;113(Pt 15):2647–58.
[36] Liu WH, Roemer SC, Port AM, Churchill ME. CAF-1-induced oligomerization of histones H3/H4 and mutually exclusive interactions with Asf1 guide H3/H4 transitions among histone chaperones and DNA. Nucleic Acids Res 2012;40:11229–39.
[37] Zhang Z, Shibahara K, Stillman B. PCNA connects DNA replication to epigenetic inheritance in yeast. Nature 2000;408:221–5.
[38] Turkewitz AP, Orias E, Kapler G. Functional genomics: the coming of age for *Tetrahymena thermophila*. Trends Genet 2002;18:35–40.
[39] Garcia BA, Hake SB, Diaz RL, Kauer M, Morris SA, Recht J, et al. Organismal differences in post-translational modifications in histones H3 and H4. J Biol Chem 2007;282:7641–55.
[40] Eisen JA, Coyne RS, Wu M, Wu D, Thiagarajan M, Wortman JR, et al. Macronuclear genome sequence of the ciliate *Tetrahymena thermophila*, a model eukaryote. PLoS Biol 2006;4:e286.
[41] Daganzo SM, Erzberger JP, Lam WM, Skordalakes E, Zhang R, Franco AA, et al. Structure and function of the conserved core of histone deposition protein Asf1. Curr Biol 2003;13:2148–58.
[42] Aury JM, Jaillon O, Duret L, Noel B, Jubin C, Porcel BM, et al. Global trends of whole-genome duplications revealed by the ciliate *Paramecium tetraurelia*. Nature 2006;444:171–8.
[43] Sillje HH, Nigg EA. Identification of human Asf1 chromatin assembly factors as substrates of Tousled-like kinases. Curr Biol 2001;11:1068–73.
[44] English CM, Adkins MW, Carson JJ, Churchill ME, Tyler JK. Structural basis for the histone chaperone activity of Asf1. Cell 2006;127:495–508.
[45] Antczak AJ, Tsubota T, Kaufman PD, Berger JM. Structure of the yeast histone H3–ASF1 interaction: implications for chaperone mechanism, species-specific interactions, and epigenetics. BMC Struct Biol 2006;6:26.
[46] Malay AD, Umehara T, Matsubara-Malay K, Padmanabhan B, Yokoyama S. Crystal structures of fission yeast histone chaperone Asf1 complexed with the Hip1 B-domain or the Cac2 C terminus. J Biol Chem 2008;283:14022–31.
[47] Tang Y, Poustovoitov MV, Zhao K, Garfinkel M, Canutescu A, Dunbrack R, et al. Structure of a human ASF1a–HIRA complex and insights into specificity of histone chaperone complex assembly. Nat Struct Mol Biol 2006;13:921–9.
[48] Min B, Collins K. An RPA-related sequence-specific DNA-binding subunit of telomerase holoenzyme is required for elongation processivity and telomere maintenance. Mol Cell 2009;36:609–19.
[49] Cassidy-Hanley D, Bowen J, Lee JH, Cole E, VerPlank LA, Gaertig J, et al. Germline and somatic transformation of mating *Tetrahymena thermophila* by particle bombardment. Genetics 1997;146:135–47.
[50] Karrer KM. Nuclear dualism. Methods Cell Biol 2012;109:29–52.
[51] Choi H, Larsen B, Lin ZY, Breitkreutz A, Mellacheruvu D, Fermin D, et al. SAINT: probabilistic scoring of affinity purification–mass spectrometry data. Nat Methods 2011;8:70–3.
[52] Choi H, Liu G, Mellacheruvu D, Tyers M, Gingras AC, Nesvizhskii AI. Analyzing protein–protein interactions from affinity purification–mass spectrometry data with SAINT. *Current protocols in bioinformatics/editorial board, Andreas D. Baxevanis ...* [et al.], Chapter 8, Unit8 15; 2012.
[53] Cook AJ, Gurard-Levin ZA, Vassias I, Almouzni G. A specific function for the histone chaperone NASP to fine-tune a reservoir of soluble H3–H4 in the histone supply chain. Mol Cell 2011;44:918–27.
[54] Chen F, Mackey AJ, Stoeckert Jr CJ, Roos DS. OrthoMCL-DB: querying a comprehensive multi-species collection of ortholog groups. Nucleic Acids Res 2006;34:D363–8.
[55] Malone CD, Falkowska KA, Li AY, Galanti SE, Kanuru RC, LaMont EG, et al. Nucleus-specific importin alpha proteins and nucleoporins regulate protein import and nuclear division in the binucleate *Tetrahymena thermophila*. Eukaryot Cell 2008;7:1487–99.
[56] Madireddi MT, Coyne RS, Smothers JF, Mickey KM, Yao MC, Allis CD. Pdd1p, a novel chromodomain-containing protein, links heterochromatin assembly and DNA elimination in *Tetrahymena*. Cell 1996;87:75–84.
[57] Martindale DW, Allis CD, Bruns PJ. Conjugation in *Tetrahymena thermophila*. A temporal analysis of cytological stages. Exp Cell Res 1982;140:227–36.
[58] Xiong J, Yuan D, Fillingham JS, Garg J, Lu X, Chang Y, et al. Gene network landscape of the ciliate *Tetrahymena thermophila*. PloS one 2011;6:e20124.

[59] Miao W, Xiong J, Bowen J, Wang W, Liu Y, Braguinets O, et al. Microarray analyses of gene expression during the *Tetrahymena thermophila* life cycle. PloS one 2009;4:e4429.
[60] Iwamoto M, Mori C, Kojidani T, Bunai F, Hori T, Fukagawa T, et al. Two distinct repeat sequences of Nup98 nucleoporins characterize dual nuclei in the binucleated ciliate *tetrahymena*. Curr Biol 2009;19:843–7.
[61] Natsume R, Eitoku M, Akai Y, Sano N, Horikoshi M, Senda T. Structure and function of the histone chaperone CIA/ASF1 complexed with histones H3 and H4. Nature 2007;446:338–41.
[62] Balaji S, Iyer LM, Aravind L. HPC2 and ubinuclein define a novel family of histone chaperones conserved throughout eukaryotes. Mol Biosyst 2009;5:269–75.
[63] Keck KM, Pemberton LF. Histone chaperones link histone nuclear import and chromatin assembly. Biochim Biophys Acta 2012;1819:277–89.
[64] Blackwell Jr JS, Wilkinson ST, Mosammaparast N, Pemberton LF. Mutational analysis of H3 and H4 N termini reveals distinct roles in nuclear import. J Biol Chem 2007;282:20142–50.
[65] Li X, Liu K, Li F, Wang J, Huang H, Wu J, et al. Structure of C-terminal tandem BRCT repeats of Rtt107 protein reveals critical role in interaction with phosphorylated histone H2A during DNA damage repair. J Biol Chem 2012;287:9137–46.
[66] Stucki M, Clapperton JA, Mohammad D, Yaffe MB, Smerdon SJ, Jackson SP. MDC1 directly binds phosphorylated histone H2AX to regulate cellular responses to DNA double-strand breaks. Cell 2005;123:1213–26.
[67] Song X, Gjoneska E, Ren Q, Taverna SD, Allis CD, Gorovsky MA. Phosphorylation of the SQ H2A.X motif is required for proper meiosis and mitosis in *Tetrahymena thermophila*. Mol Cell Biol 2007;27:2648–60.
[68] Tamburini BA, Carson JJ, Adkins MW, Tyler JK. Functional conservation and specialization among eukaryotic anti-silencing function 1 histone chaperones. Eukaryot Cell 2005;4:1583–90.
[69] Wurtele H, Tsao S, Lepine G, Mullick A, Tremblay J, Drogaris P, et al. Modulation of histone H3 lysine 56 acetylation as an antifungal therapeutic strategy. Nat Med 2010;16:774–80.
[70] Peterson DS, Gao Y, Asokan K, Gaertig J. The circumsporozoite protein of *Plasmodium falciparum* is expressed and localized to the cell surface in the free-living ciliate *Tetrahymena thermophila*. Mol Biochem Parasitol 2002;122:119–26.
[71] Fillingham JS, Bruno D, Pearlman RE. Cis-acting requirements in flanking DNA for the programmed elimination of mse2.9: a common mechanism for deletion of internal eliminated sequences from the developing macronucleus of *Tetrahymena thermophila*. Nucleic Acids Res 2001;29:488–98.
[72] Krogan NJ, Cagney G, Yu H, Zhong G, Guo X, Ignatchenko A, et al. Global landscape of protein complexes in the yeast *Saccharomyces cerevisiae*. Nature 2006;440:637–43.
[73] Kean MJ, Couzens AL, Gingras AC. Mass spectrometry approaches to study mammalian kinase and phosphatase associated proteins. Methods 2012;57:400–8.
[74] Liu G, Zhang J, Larsen B, Stark C, Breitkreutz A, Lin ZY, et al. ProHits: integrated software for mass spectrometry-based interaction proteomics. Nat Biotechnol 2010;28:1015–7.
[75] Gorovsky MA. Studies on nuclear structure and function in *Tetrahymena pyriformis*. II. Isolation of macro- and micronuclei. J Cell Biol 1970;47:619–30.
[76] Fillingham JS, Pearlman RE. Role of micronucleus-limited DNA in programmed deletion of mse2.9 during macronuclear development of *Tetrahymena thermophila*. Eukaryot Cell 2004;3:288–301.
[77] Fillingham JS, Garg J, Tsao N, Vythilingum N, Nishikawa T, Pearlman RE. Molecular genetic analysis of an SNF2/brahma-related gene in *Tetrahymena thermophila* suggests roles in growth and nuclear development. Eukaryot Cell 2006;5:1347–59.
[78] Wenkert D, Allis CD. Timing of the appearance of macronuclear-specific histone variant hv1 and gene expression in developing new macronuclei of *Tetrahymena thermophila*. J Cell Biol 1984;98:2107–17.
[79] Gautier L, Cope L, Bolstad BM, Irizarry RA. AFFY—analysis of Affymetrix GeneChip data at the probe level. Bioinformatics 2004;20:307–15.
[80] Faith JJ, Hayete B, Thaden JT, Mogno I, Wierzbowski J, Cottarel G, et al. Large-scale mapping and validation of *Escherichia coli* transcriptional regulation from a compendium of expression profiles. PLoS Biol 2007;5:e8.